Carbon Nanotubes Coupled with Layered Graphite to Support SnTe Nanodots as High-Rate and Ultra-Stable Lithium Ion Battery Anodes

Huanhui Chen[1,a,b], Guanxia Ke[1,a], Xiaochao Wu[1,a], Wanqing Li [a], Hongwei Mi [a], Yongliang Li [a], Lingna Sun [a], Qianling Zhang [a], Chuanxin He [a], Xiangzhong Ren [a,*]

[a] College of Chemistry and Environmental Engineering, Shenzhen University, Shenzhen, Guangdong 518060, P.R. China

[b] Shenzhen Engineering Lab of Flexible Transparent Conductive Films, School of Materials Science and Engineering, Harbin Institute of Technology, Shenzhen 518055, China

***Corresponding author.**

Xiangzhong Ren, Email: renxz@szu.edu.cn, Tel/Fax: +86-755-26558134

[1] These authors contributed equally to this work.

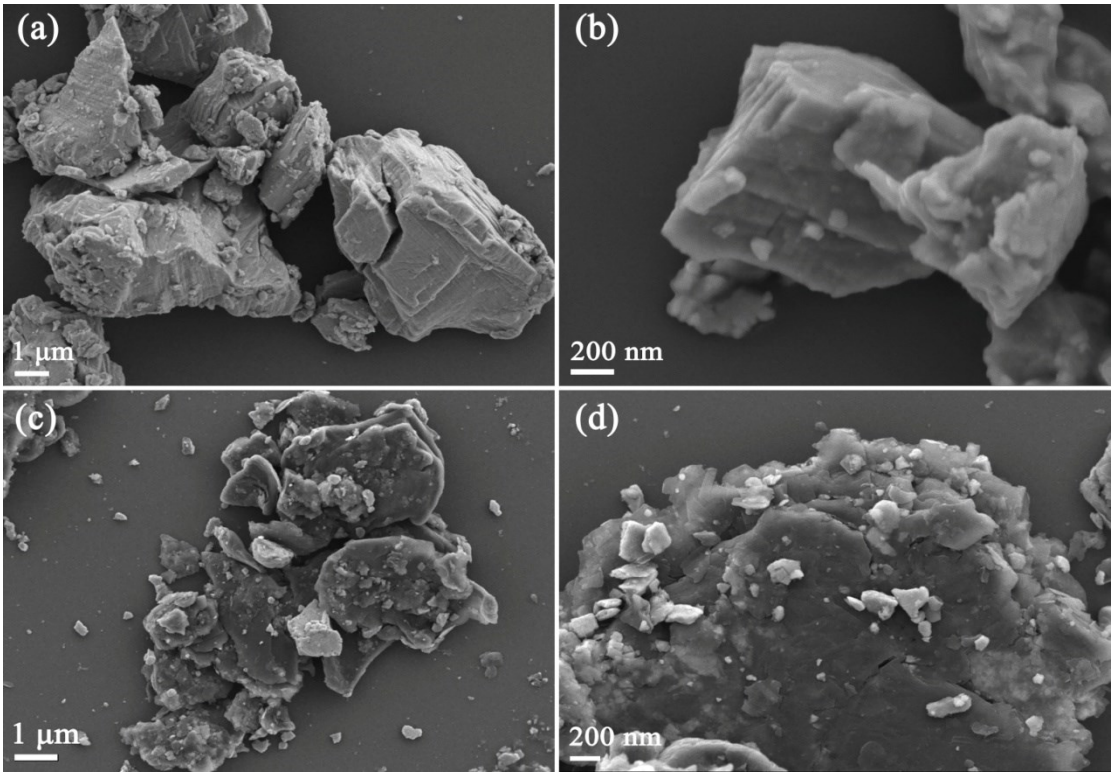

Fig. S1 (a-b) The SEM images of pure SnTe at different magnification. (c-d) The SEM images of SnTe-G at different magnification.

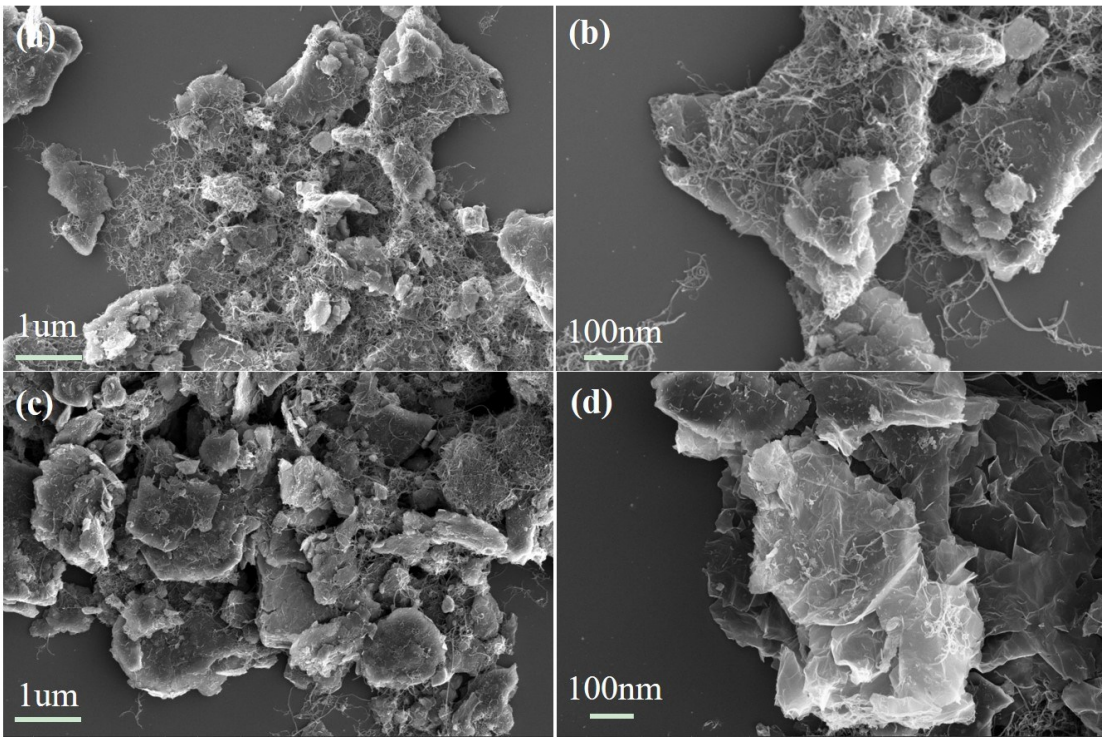

Fig. S2 (a-b) The SEM images of SnTe-CNT-G-0.6 different magnification. (c-d) The SEM images of SnTe-CNT-G-1.0 at different magnification.

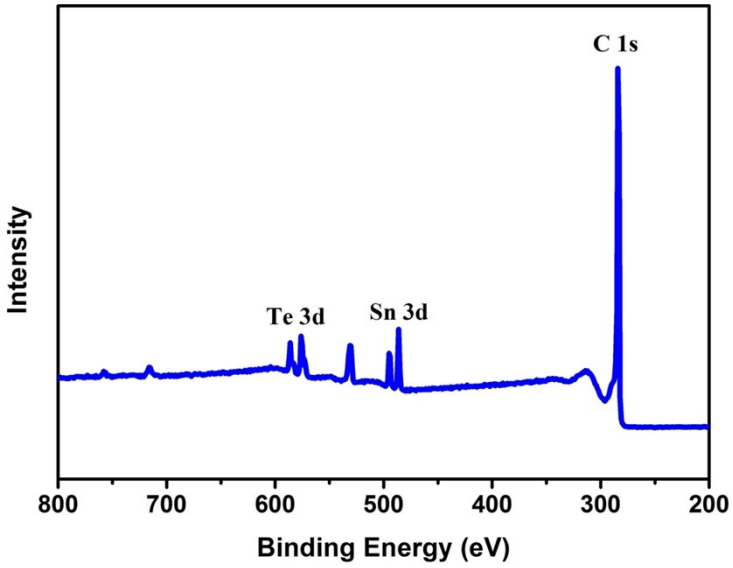

Fig. S3 XPS survey-scan spectra of SnTe-CNT-G.

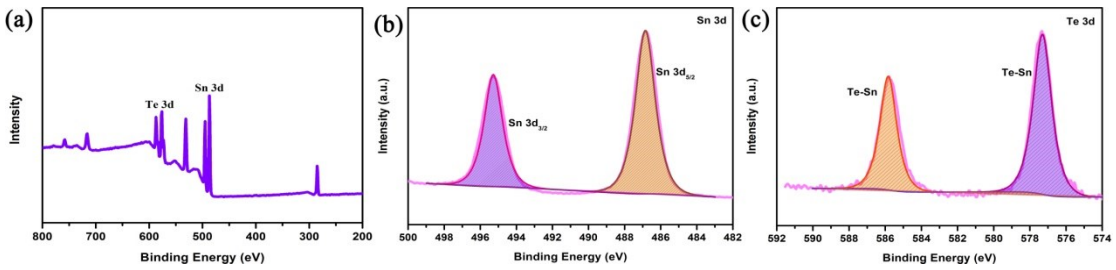

Fig. S4 XPS survey-scan spectra of SnTe (a), Core level spectra of Sn 3d (b) and Te 3d (c).

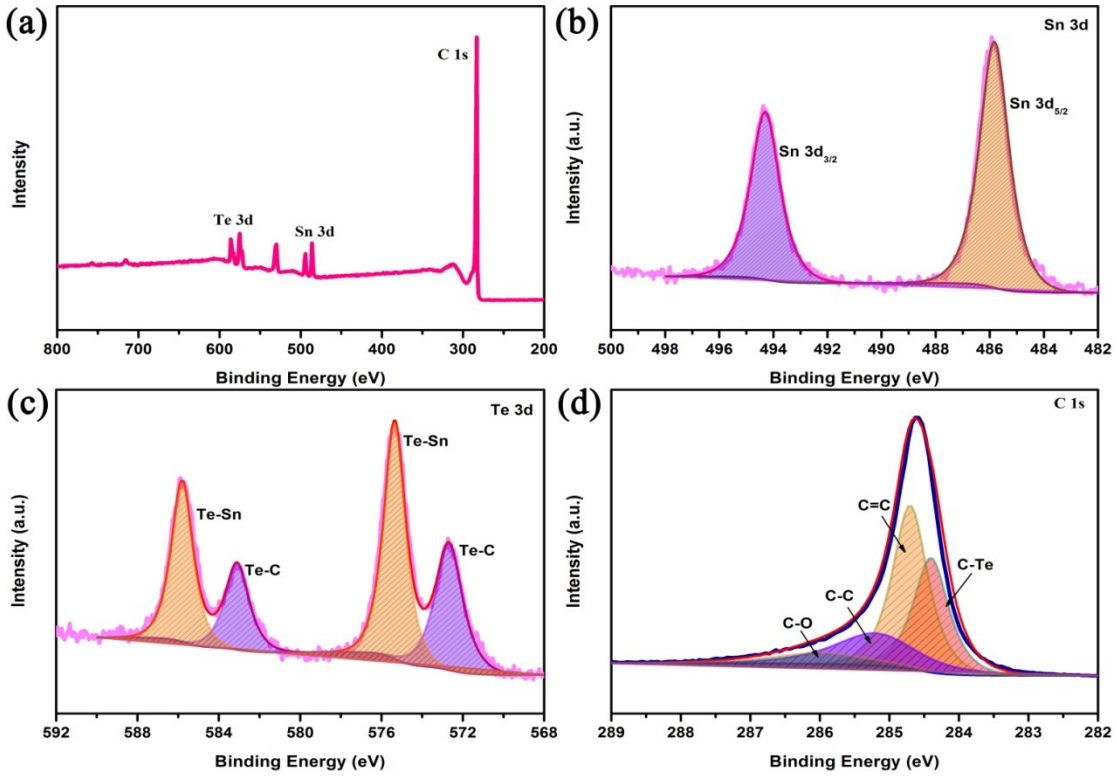

Fig. S5 XPS survey-scan spectra of SnTe-G (a), Core level spectra of Sn 3d (c), Te 3d (d) and C 1s (e).

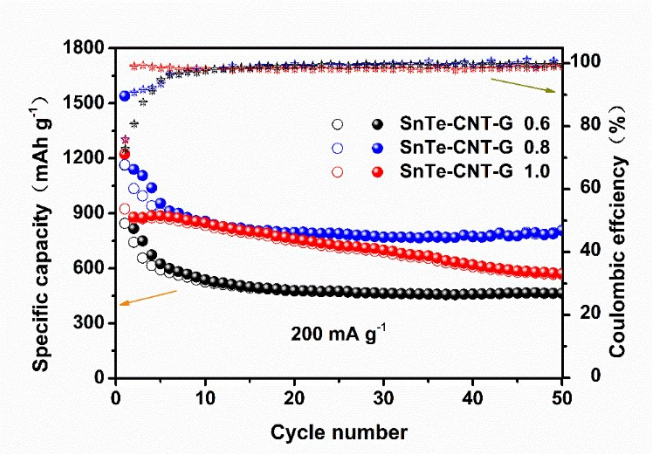

Fig. S6 Cycling performance and Coulomb efficiency of SnTe-CNT-G with different graphite content at 200 mA g^{-1}.

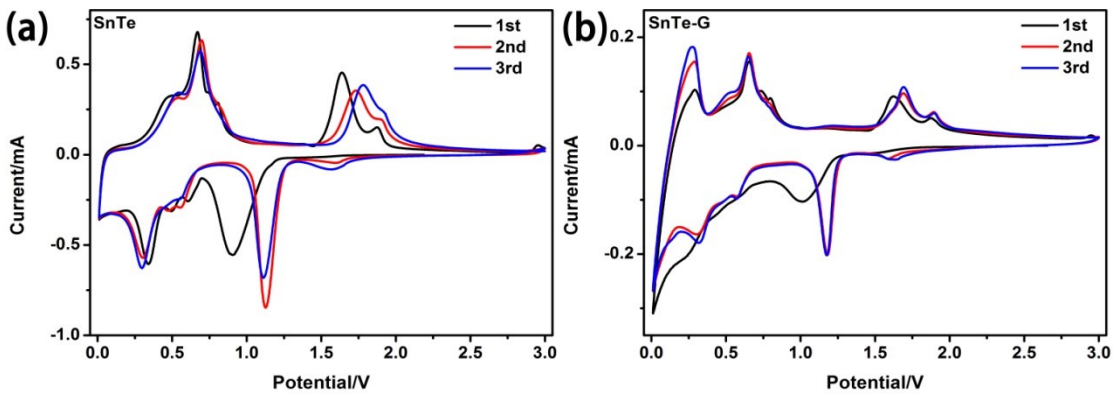

Fig. S7 (a) CV curves of the SnTe-CNT-G anodes at 0.2 mV/s; (b) CV curves of the SnTe-CNT-G anodes at 0.2 mV/s.

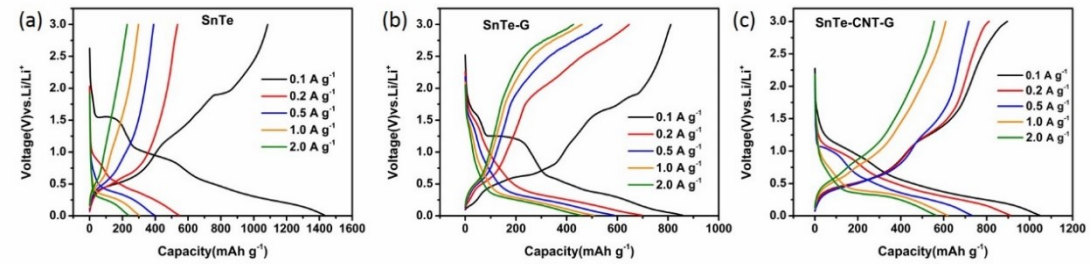

Fig.S8 The galvanostatic charge-discharge profiles at varied current density of a) SnTe; b) SnTe-G; c) SnTe-CNT-G.

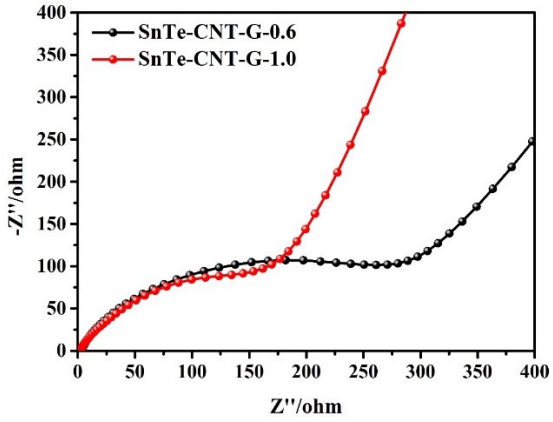

Fig. S9 Nyquist plots of SnTe-CNT-G with different graphite content.

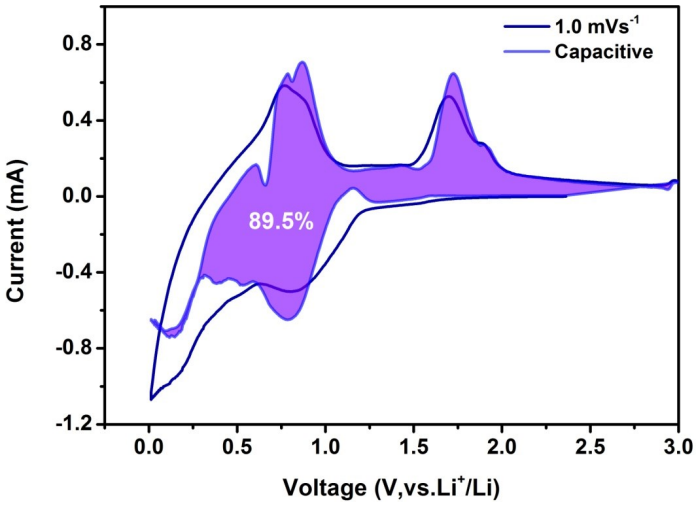

Fig. S10 The pseudocapacitance contribution ratios of the SnTe-CNT-G electrodes at a scan rate of 1 mV s^{-1}.

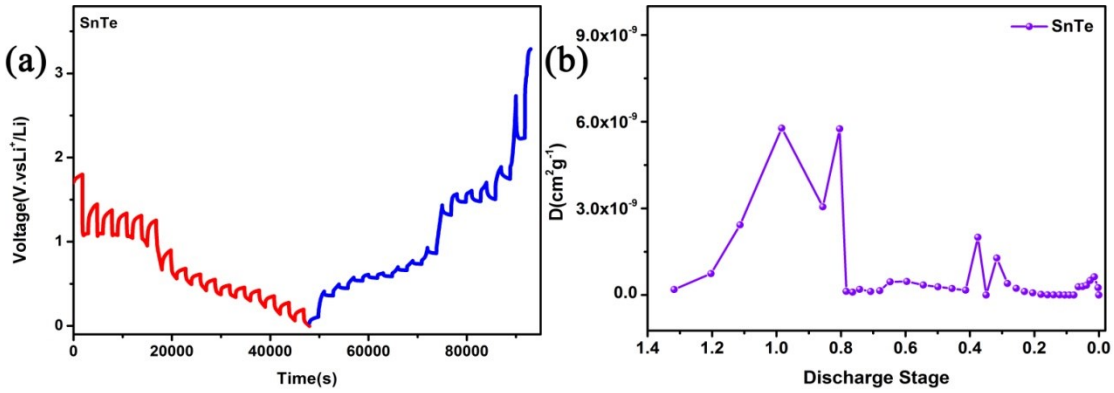

Fig. S11 GITT curves of the SnTe electrode (a) and their Li^+ diffusion coefficient for the initial discharge states (b).

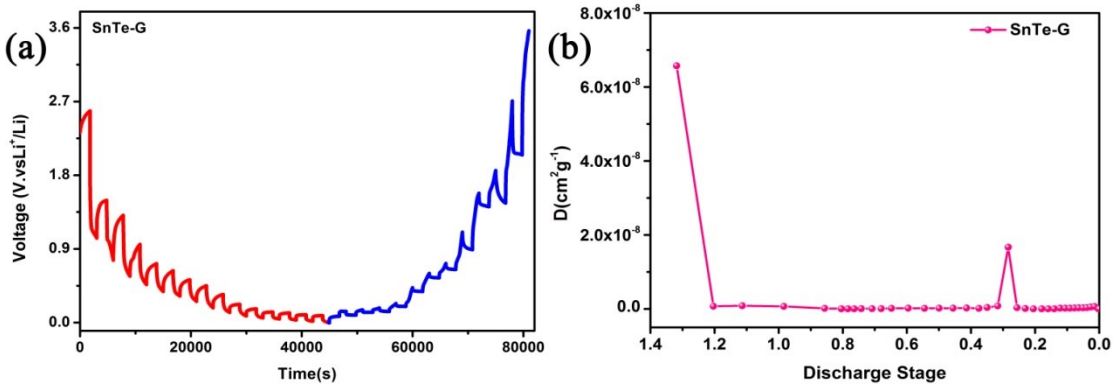

Fig. S12 GITT curves of the SnTe-G electrode (a) and their Li^+ diffusion coefficient for the initial discharge states (b).

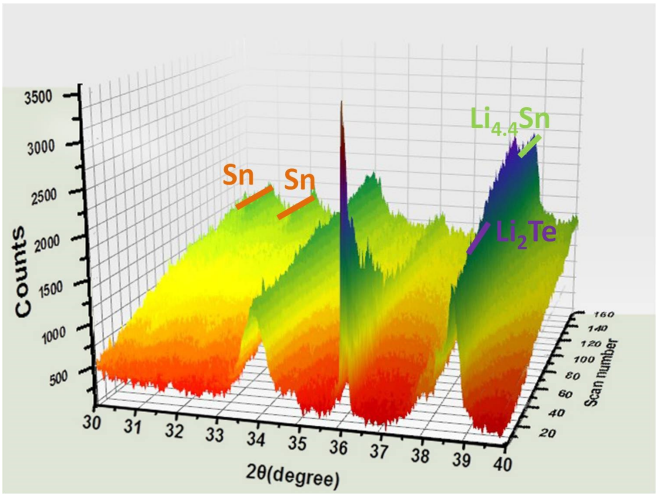

Fig. S13 3D contour plots of in-situ XRD patterns for SnTe-CNT-G anodes during the initial cycle.

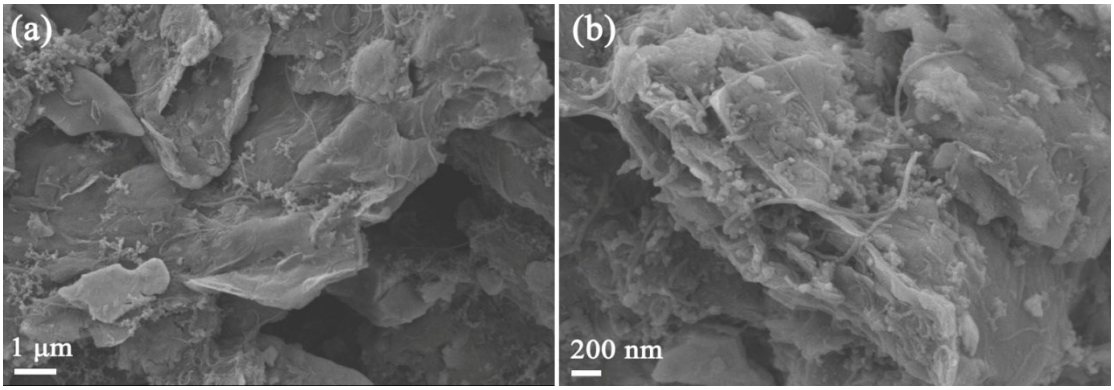

Fig. S14 (a-b) SEM images of SnTe-CNT-G electrode before cycling.

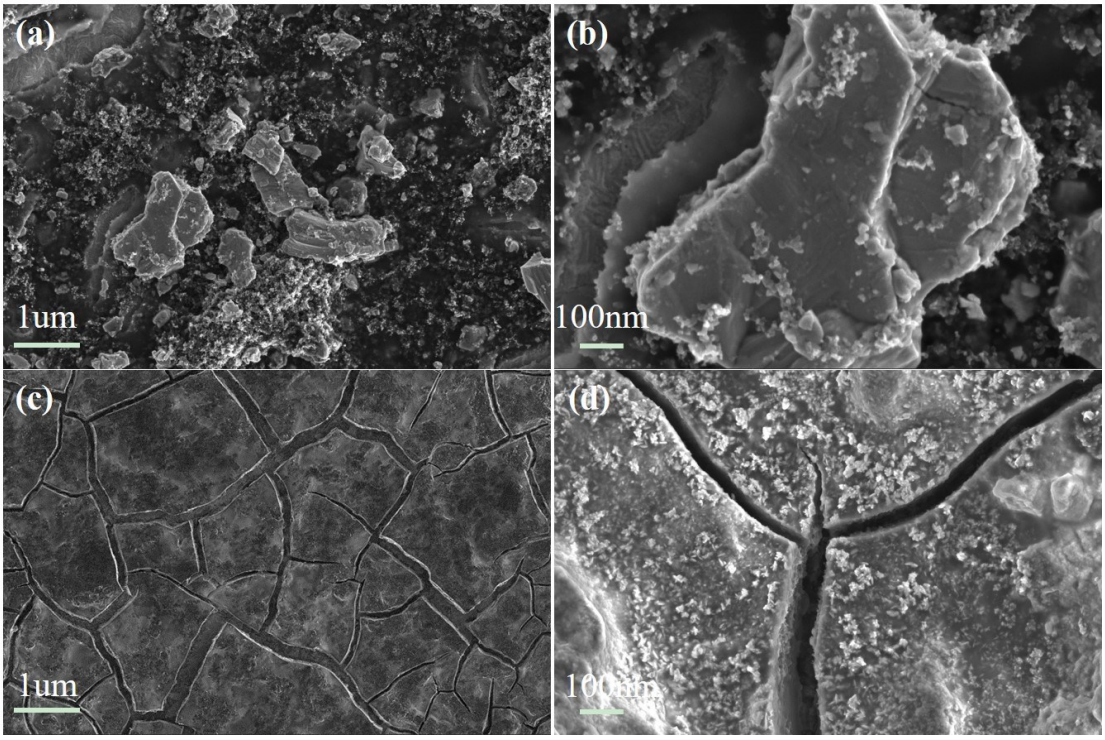

Fig. S15 (a-b) SEM images of SnTe electrode before cycling; (c-d) SEM images of SnTe electrode at 200 mA g^{-1} after 100 cycles.

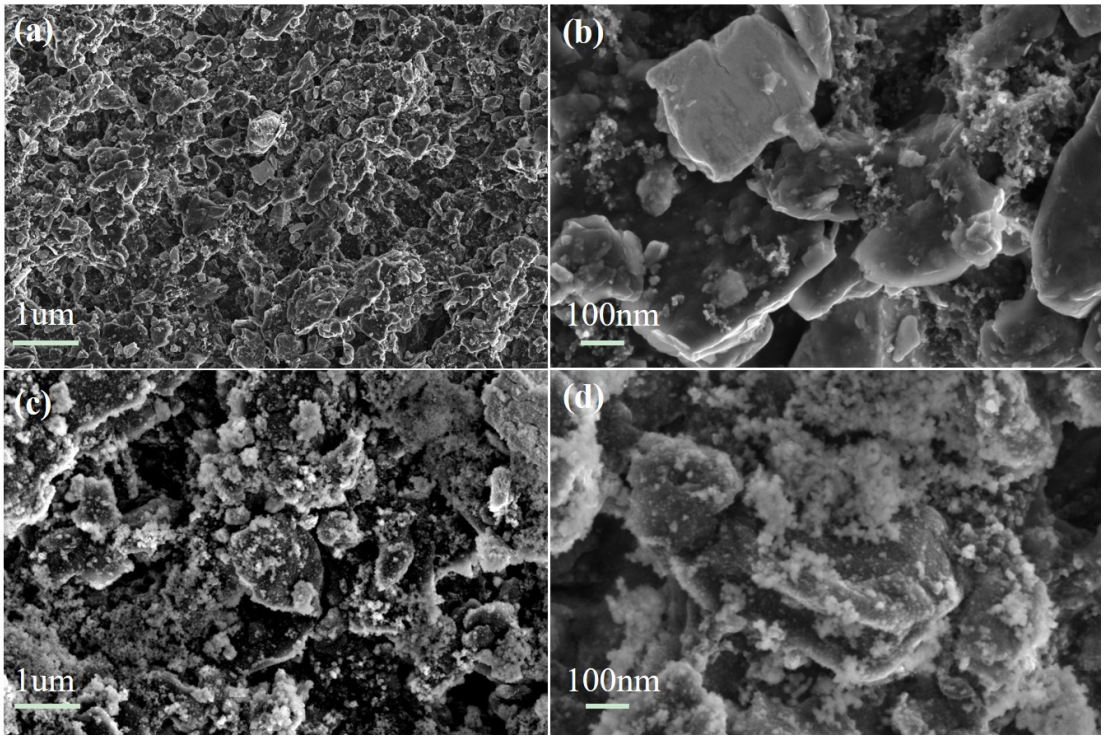

Fig. S16 (a-b) SEM images of SnTe-G electrode before cycling; (c-d) SEM images of SnTe-G electrode at 200 mA g^{-1} after 100 cycles.

Table S1. Comparison of the electrochemical lithium storage performance of the SnTe-CNT-G electrodes with the literature data.

Materials	Reversible capacity ($mAhg^{-1}$)/Cycle number				Ref.
	Current density 100mA g^{-1}	**Current density 200mA g^{-1}**	**Current density 1000mA g^{-1}**	**Current density 2000mA g^{-1}**	
Sb_2Te_3@Gra	570/200th			372/200th	[1]
$SnSb_2Te_4$/G		574/100th	478/1000th		[2]
$MoTe_2$/FLG	674/150th			335/10th	[3]
$Ge_2Sb_2Te_5$	947/100th			546/10th	[4]
$SnSe_2$ QDs/rGO		746/500th		460/3000th	[5]
C/SnO/Sn	816/100th		504/1000th		[6]
SnS/CNFs		648/500th	520/2400th	167/10th	[7]
Sn/NMCs		472/500th	437/1600th		[8]
SnO_2/ Ti_3C_2			530/500th	489/10th	[9]
SnO_2 QDs/$Ti_3C_2T_x$	660/100th		522/10th	410/10th	[10]
SnTe-CNT-G		**840/100th**		**669/1400th**	**This work**

References

1. Y. Wei, J. Chen, S. Wang, X. Zhong, R. Xiong, L. Gan, Y. Ma, T. Zhai and H. Li, *ACS Applied Materials Interfaces*, 2020, **12**, 16264-16275.
2. Z. Wu, G. Liang, W. K. Pang, T. Zhou, Z. Cheng, W. Zhang, Y. Liu, B. Johannessen and Z. Guo, *Advanced Materials*, 2020, **32**, e1905632.
3. N. Ma, X. Y. Jiang, L. Zhang, X. S. Wang, Y. L. Cao and X. Z. Zhang, *Small*, 2018, **14**, e1703680.
4. Y. Wei, L. Huang, J. Chen, Y. Guo, S. Wang, H. Li and T. Zhai, *ACS Applied Materials Interfaces*, 2019, **11**, 41374-41382.

5. Z. Xiang Huang, B. Liu, D. Kong, Y. Wang and H. Ying Yang, *Energy Storage Materials*, 2018, **10**, 92-101.
6. Y. Cheng, Z. Yi, C. Wang, Y. Wu and L. Wang, *Chemical Engineering Journal*, 2017, **330**, 1035-1043.
7. J. Xia, L. Liu, S. Jamil, J. Xie, H. Yan, Y. Yuan, Y. Zhang, S. Nie, J. Pan, X. Wang and G. Cao, *Energy Storage Materials*, 2019, **17**, 1-11.
8. H. Ying, S. Zhang, Z. Meng, Z. Sun and W.-Q. Han, *Journal of Materials Chemistry A*, 2017, **5**, 8334-8342.
9. Y. T. Liu, P. Zhang, N. Sun, B. Anasori, Q. Z. Zhu, H. Liu, Y. Gogotsi and B. Xu, *Advanced Materials*, 2018, **30**, e1707334.
10. H. Liu, X. Zhang, Y. Zhu, B. Cao, Q. Zhu, P. Zhang, B. Xu, F. Wu and R. Chen, *Nano-Micro Letters*, 2019, **11**.